Peroxisome-Generated Hydrogen Peroxide as Important Mediator of Lipotoxicity in Insulin-Producing Cells

Matthias Elsner, Wiebke Gehrmann, and Sigurd Lenzen

OBJECTIVE—Type 2 diabetes is a complex disease that is accompanied by elevated levels of nonesterified fatty acids (NEFAs), which contribute to β-cell dysfunction and β-cell loss, referred to as lipotoxicity. Experimental evidence suggests that oxidative stress is involved in lipotoxicity. In this study, we analyzed the molecular mechanisms of reactive oxygen species–mediated lipotoxicity in insulin-producing RINm5F cells and INS-1E cells as well as in primary rat islet cells.

RESEARCH DESIGN AND METHODS—The toxicity of saturated NEFAs with different chain lengths upon insulin-producing cells was determined by MTT and propidium iodide (PI) viability assays. Catalase or superoxide dismutase overexpressing cells were used to analyze the nature and the cellular compartment of reactive oxygen species formation. With the new H_2O_2-sensitive fluorescent protein HyPer H_2O_2 formation induced by exposure to palmitic acid was determined.

RESULTS—Only long-chain (>C14) saturated NEFAs were toxic to insulin-producing cells. Overexpression of catalase in the peroxisomes and in the cytosol, but not in the mitochondria, significantly reduced H_2O_2 formation and protected the cells against palmitic acid–induced toxicity. With the HyPer protein, H_2O_2 generation was directly detectable in the peroxisomes of RINm5F and INS-1E insulin-producing cells as well as in primary rat islet cells.

CONCLUSIONS—The results demonstrate that H_2O_2 formation in the peroxisomes rather than in the mitochondria are responsible for NEFA-induced toxicity. Therefore, we propose a new concept of fatty acid–induced β-cell lipotoxicity mediated via reactive oxygen species formation through peroxisomal β-oxidation.

Type 2 diabetes is a complex metabolic syndrome characterized by peripheral insulin resistance and pancreatic β-cell dysfunction (1,2), resulting in defective glucose-induced insulin secretion (3–5) and β-cell dysfunction and loss through apoptosis (6–8). Obesity and the metabolic syndrome typically precede diabetes manifestation, which is accompanied by elevated levels of nonesterified fatty acids (NEFAs) (9). NEFA elevation can suppress insulin secretion and cause β-cell dysfunction, which may ultimately lead to β-cell loss, a phenomenon referred to as lipotoxicity (10,11).

The costs of publication of this article were defrayed in part by the payment of page charges. This article must therefore be hereby marked "advertisement" in accordance with 18 U.S.C. Section 1734 solely to indicate this fact.

Saturated long-chain fatty acids are toxic to primary β-cells and insulin-producing cell lines (12,13). However, the molecular mechanisms underlying lipotoxicity are only partially understood (14,15). Recent evidence suggested that lipotoxic β-cell damage is accompanied by endoplasmic reticulum (ER) stress and calcium depletion in the ER, ultimately leading to β-cell apoptosis via caspase activation (16). On the other hand, the fact that nonmetabolizable methylated fatty acids are nontoxic and induce little or no ER stress provides an indication for the necessity of fatty acid metabolism to the toxic action (15,17). In 2008, Lai et al. (18) showed that overexpression of the ER chaperone Bip could not protect against palmitic acid–induced toxicity, supporting the argument against ER stress as the main molecular mechanism of lipotoxicity.

NEFA catabolism via mitochondrial β-oxidation is an important source of energy for pancreatic β-cells (19–21). It has been proposed that increased β-oxidation and oxidative phosphorylation cause lipotoxicity by enhancing formation of reactive oxygen species (ROS) in the mitochondria (15). Superoxide radicals are generated at complexes I and III of the respiratory chain (22) and can give rise to toxic hydrogen peroxide (H_2O_2) and hydroxyl radicals (23,24). Interestingly, some studies have suggested that mitochondrial β-oxidation can be protective, whereas inhibition of β-oxidation increases lipotoxicity (25,26). However, neither concept fully explains the molecular mechanism of lipotoxicity.

Herein, we provide experimental evidence in support of an entirely new concept of NEFA-induced β-cell lipotoxicity based on peroxisomal metabolism of NEFAs. Long-chain NEFAs, such as palmitic and stearic acid, can be metabolized through β-oxidation in the peroxisomes as well as in the mitochondria (27,28). In contrast to mitochondrial β-oxidation, the acyl-CoA oxidases in the peroxisomes form H_2O_2 and not reducing equivalents (28). For H_2O_2 inactivation, the oxidoreductase catalase is typically expressed in peroxisomes (28). However, expression of H_2O_2-inactivating catalase is virtually absent in the peroxisomes of insulin-producing cells (29,30). This lack of a low-affinity, high-capacity H_2O_2-inactivating enzyme (29,30) impedes inactivation of peroxisome-generated H_2O_2, thereby increasing the vulnerability of pancreatic β-cells to ROS-mediated lipotoxicity (15,23).

RESEARCH DESIGN AND METHODS

Tissue culture of insulin-producing cells. Insulin-producing RINm5F cells and INS-1E cells (provided by C. Wollheim) were cultured as described previously (30,31).

RINm5F cell clones that overexpressed different antioxidative enzymes were generated as described previously (32,33). Cellular expression of antioxidative enzymes was analyzed by Western blot or catalase enzyme activity measurement (33).

For the quantification of the catalase activity, the method originally described by Claiborne (34) was used. In brief, cells were homogenized in PBS (pH 7.4) through sonication on ice for 1 min in 15-s bursts at 90 watts. Catalase

activity was measured by ultraviolet spectroscopy, monitoring the decomposition of H_2O_2 at 240 nm. Catalase activity was calculated by the following equation:

$$U/mg = \frac{\Delta A \cdot min^{-1} \cdot 1000 \cdot ml\ Reaction\ Mix}{43.6 \cdot mg\ Protein}$$

NEFAs (Sigma, St. Louis, MO) were dissolved in 90% ethanol heated to 60°C and used at different concentrations in RPMI 1640 (PAN, Aidenbach, Germany) with 1% FCS and a final BSA (MP Biomedicals, Eschwege, Germany): NEFA ratio of 2%: 1 nmol/l, according to Cnop et al. (13). All control wells received the same amount of solvent and BSA. This procedure did not cause a significant decrease in viability in the absence of added fatty acids.

Rat islet isolation and culture. Pancreatic islets were isolated from 250–300 g adult male Lewis rats by collagenase digestion, separated by Ficoll gradient, and handpicked under a stereo microscope. Isolated islets were cultured on extracellular matrix (ECM)-coated plates (35 mm) (Novamed, Jerusalem, Israel, the ECM being derived from bovine corneal endothelial cells) in RPMI-1640 medium containing 5 mmol/l glucose, 10% FCS, penicillin, and streptomycin at 37°C in a humidified atmosphere of 5% CO_2 according to Cornu et al. (35). The islets were cultured for 7–10 days on the ECM plates to adhere and spread before they were infected with HyPer-Peroxi lentivirus or treated with palmitic acid.

Assessment of cell viability. RINm5F mock-transfected and cytoprotective enzyme overexpressing RINm5F insulin-producing cells were seeded at 25,000 cells/well in 100-μl culture medium in 96-well plates (for propidium iodide [PI] staining, black 96-well plates) and allowed to attach for 24 h before they were incubated at 37°C with NEFAs for 24 h. Cell viability was then determined by either microplate-based MTT assay (3-(4,5-dimethylthiazol-2-yl)-2,5-diphenyl tetrazolium bromide) (36) or PI staining (Sigma, St. Louis, MO). PI is membrane impermeant and usually excluded from viable cells (37). To measure the rate of cell death after NEFA treatment, the PI stock solution (12.5 μg/ml) was diluted in the incubation media to a final concentration of 0.625 μg/ml. After 15 min incubation in the dark, the plates were analyzed at 520/620 nm excitation/emission using the fluorescence reader Victor² 1420 Multilabel Counter (Perkin Elmer, Wiesbaden, Germany).

Determination of oxidative stress by DCF-DA fluorescence. To detect overall oxidative stress, 25,000 cells were seeded in 96-well black plates and cultured for 24 h. The cells were then preincubated with 10 μmol/l DCF-DA (2, 7-dichlorofluorescein diacetate, Sigma, St. Louis, MO) for 30 min at 37°C. Thereafter, medium containing dichlorofluorescein diacetate (DCF-DA) was replaced with fresh medium with or without palmitic acid. After a 24-h incubation, the plates were analyzed at 480/520 nm excitation/emission using the fluorescence reader Victor² 1420 Multilabel Counter (Perkin Elmer, Wiesbaden, Germany) (38). Data are expressed as percentages relative to untreated cells.

Cloning of HyPer vectors. For in vivo analyses of mitochondrial H_2O_2 generation, the cDNA of the H_2O_2-sensitive fluorescent HyPer protein (39) was subcloned from the pHyPer-dMito (Evrogen, Moscow, Russia) into the lentiviral transfer plasmid pLenti6/V5-MCS (Invitrogen, Karlsruhe, Germany). The cDNA was excised from the pHyPer-dMito plasmid using the NheI and NotI restriction sites, blunted, and ligated into the EcoRV site of the pLenti6/V5-MCS plasmid. To construct the expression vector for the HyPer-Peroxi protein, the peroxisome target signal (PTS1) (40,41) was joined to the 3′-end of the HyPer cDNA by PCR using composite primer (HyPer-PTS1-XbaI-fw (5′-TATCTAGACGCCACCATGGAGATGGCAA-3′) and HyPer-PTS1-Bsp119I-rv (5′-GCTTCGAATTACAGCTTGGAAACCGCCTGTTTTAAAAC-3′)) and the pHyPer-dCyto plasmid as template. Then, the HyPer-Peroxi cDNA was subcloned into the XbaI/Bsp119I site of the pLenti6/V5-MCS plasmid.

Preparation of lentiviruses. To express the HyPer-Mito and HyPer-Peroxi proteins, lentivirus was prepared as previously described (42): 500,000 293FT cells were transfected with the packaging plasmid pPAX2 (37.5 μg), the envelope plasmid pcDNA-MDG (7.5 μg), and the transfer plasmids pLenti6/ V5-MCS-HyPer-Mito or pLenti6/V5-MCS-HyPer-Peroxi (25 μg) by calcium phosphate precipitation. The virus particles were harvested from the culture medium 48 h later and purified by ultracentrifugation (2 h at 70,000 g). The virus titers (3–5 × 10⁷ infectious particles) were quantified by Taqman qPCR assay as described elsewhere (43).

Lentiviral transduction. The RINm5F-control, RINm5F-Cat, RINm5F-Mito-Cat (33), INS-1E, and primary rat islet cells were infected with HyPer-Mito or HyPer-Peroxi lentivirus at a MOI of 10. The tissue culture cells were selected for HyPer expression using blasticidin (1 μmol/l).

Analysis of H_2O_2 generation using HyPer proteins. RINm5F cells or primary rat islet cells that overexpressed HyPer-Mito or HyPer-Peroxi were seeded onto black 24-well glass-bottom plates (Greiner, Frickenhausen, Germany). Cells were cultured for 24 h and afterward exposed to palmitic acid for another 24 h. Live cell imaging was performed using a CFP-YFP dual filter

(excitation, 427 nm and 504 nm; emission, 520 nm) with a cellʀ/Olympus IX 81 inverted microscope system and CellR software (Olympus, Hamburg, Germany) for imaging and analysis.

To determine H_2O_2 production, changes in the fluorescence ratios of RINm5F, RINm5F-Cat, RINm5F-MitoCat, and INS-1E cells that overexpressed HyPer-Mito or HyPer-Peroxi were quantified spectrofluorometrically. Those cells were seeded at 25,000 cells per well onto black 96-well plates and cultured for 24 h. The fluorescence ratio was measured immediately before and after 24 h treatment with palmitic acid.

Immunocytochemical staining. For immunocytochemical staining of primary rat β-cells, HepG2 cells, RINm5F cells, and RINm5F cells that overexpressed catalase, 100,000 cells were seeded overnight on collagen-coated glass slides and subsequently fixed with 4% paraformaldehyde. After washing, the cells were permeabilized and blocked with PBS containing 0.2% Triton X-100 and 1% BSA. The slides were incubated with primary antibodies (for detailed information see supplementary Table S1 in the online appendix at http:// diabetes.diabetesjournals.org/cgi/content/full/db09-1401/DC1) diluted in PBS containing 0.1% Triton X-100 and 0.1% BSA at room temperature for 60 min. Then, the cells were washed with PBS and incubated with secondary antibodies (for detailed information see supplementary Table S1) for 60 min. For nuclear counterstaining, 300 nmol/l DAPI was applied for 5 min at room temperature. Finally, the cells were washed and mounted with Mowiol/ DABCO (Sigma, St. Louis, MO) antiphotobleaching mounting media. Stained cells were examined on an Olympus IX81 inverted microscope (Olympus, Hamburg, Germany) and microscopic images were postprocessed using AutoDeblur and AutoVisualize (Autoquant Imaging, NY).

Statistical analysis. Data are expressed as means ± SEM. Statistical analyses were performed using ANOVA plus the Dunnett test for multiple comparisons, unless stated otherwise. EC_{50} values were calculated from nonlinear regression analyses using least square algorithms of the Prism analysis program (Graphpad, San Diego, CA).

RESULTS

Chain length-dependent toxicity of saturated non-esterified fatty acids in insulin-producing cells. Saturated NEFAs were toxic to RINm5F insulin-producing cells. In both the MTT cell viability and the propidium iodide (PI) cytotoxicity assays, toxicity was dependent on NEFA chain length (Fig. 1). The longest chain length fatty acid analyzed, stearic acid (C18:0), was the most toxic, with a half-maximal effective concentration (EC_{50}) below 100 μmol/l. The EC_{50} for palmitic acid (C16:0), the physiologically most abundant and important saturated NEFA, was around 100 μmol/l after a 24-h incubation. Toxicity decreased with decreasing chain length. Myristic acid (C14:0) was highly toxic ($EC_{50} \cong 200$ μmol/l), whereas tridecanoic acid (C13:0) was significantly less toxic, with an EC_{50} well above 500 μmol/l. With further chain length shortening (C12:0 to C10:0), toxicity was negligible with EC_{50} values exceeding 1,000 μmol/l. For even shorter chain saturated fatty acids (C8:0 to C4:0), EC_{50} values could not be calculated because of marginal toxicity (data not shown). Toxicity was also observed in a fluorescence-activated cell sorter (FACS)-based caspase-3 assay (30% caspase-3 positive cells at 100 μmol/l palmitic acid as compared with 6% caspase-3 positive cells under control conditions), indicating an apoptotic mode of fatty acid-induced cell death.

Palmitic acid-induced cell death was also observed in isolated primary rat islet cells in the propidium iodide cytotoxicity assay. After a 24-h incubation with 500 μmol/l palmitic acid, 33 ± 4% of rat islet cells stained positive for propidium iodide, whereas in untreated cells the cell death rate was low (6 ± 1%).

Intracellular localization and enzyme activity of catalase in RINm5F insulin-producing cells overexpressing catalase. Although primary rat islet cells as well as untransfected RINm5F insulin-producing cells showed virtually no immunostaining for catalase (data not shown), RINm5F insulin-producing cells transfected to overex-
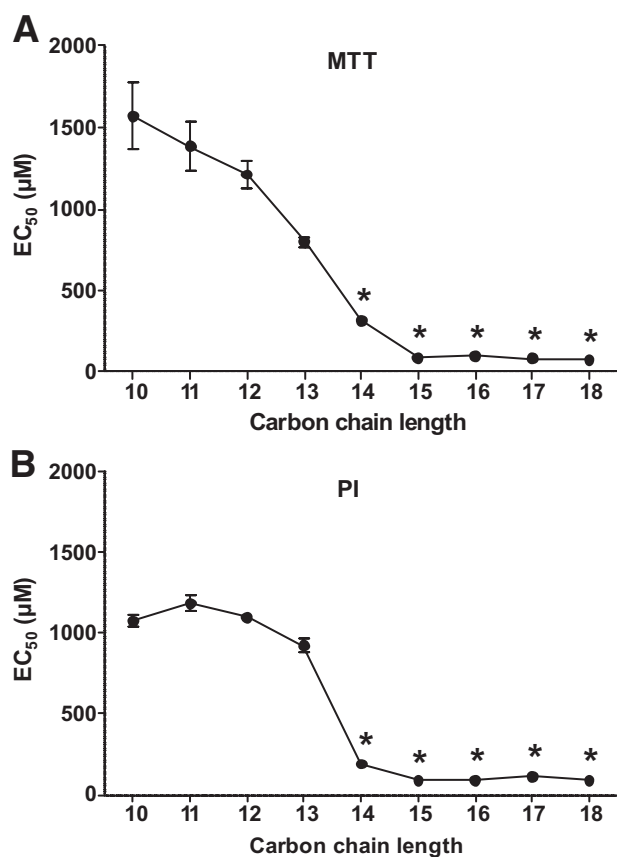
FIG. 1. Toxicity of saturated NEFAs according to chain length (C10:0-C18:0) in RINm5F insulin-producing cells. Cells were incubated for 24 h with saturated NEFAs of different chain lengths and viability was determined by MTT assay (*A*) or propidium iodide staining (*B*). EC$_{50}$ values were calculated by nonlinear regression analysis. Data are means ± SEM from 4–6 individual experiments. *$P < 0.01$ as compared with C10:0, C11:0, C12:0, or C13:0. Other comparisons were not significant (ANOVA/Tukey test for multiple comparisons).

press catalase in the cytosol (Cat) showed a homogenous distribution of catalase in the cytoplasm and a dot-like pattern of catalase colocalization with peroxisomes (Fig. 2*A*); on the other hand, catalase did not colocalize with mitochondria (Fig. 2*B*). Catalase was not detectable in the cytoplasm or in the peroxisomes of insulin-producing cells that overexpressed catalase in the mitochondria (Mito-Cat; Fig. 2*C*); in these cells, catalase colocalized specifically with the mitochondria (Fig. 2*D*).

The localization of catalase in RINm5F-Cat cells was additionally analyzed in three dimensional (3D) images using Imaris software (Bitplane, Zurich, Switzerland). The 3D models were generated from 20 z-layers of the immunocytochemical staining of catalase and the peroxisomes (supplementary Fig. S1) or the mitochondria (supplementary Fig. S2). In these images, catalase showed a clear colocalization with the peroxisomes, whereas no significant colocalization was detectable with the mitochondria.

The results of these immunostainings were also reflected by the catalase enzyme activities of the examined cells. Primary rat islet cells and untransfected RINm5F cells showed a comparable catalase activity of 20 ± 5 units/mg and 13 ± 1 unit/mg, respectively. By contrast in RINm5F-catalase (353 ± 7 units/mg) and RINm5F-mito-catalase (367 ± 43 units/mg) cells the enzyme activity was ~17-fold higher.

Effects of the antioxidative enzymes catalase and SOD on palmitic acid toxicity in insulin-producing cells. RINm5F insulin-producing cells that overexpressed different antioxidative enzymes were used as a tool to analyze the role of ROS in palmitic acid toxicity. Although overexpression of the H$_2$O$_2$-inactivating enzyme catalase in peroxisomes and in the cytosol (Cat) protected against palmitic acid (100 μmol/l) toxicity, catalase overexpression in the mitochondria (Mito-Cat) did not provide protection (Fig. 3).

Neither overexpression of the cytosolic superoxide radical detoxifying isoenzyme CuZnSOD (copper zinc superoxide dismutase) nor overexpression of the mitochondrial isoenzyme MnSOD (manganese superoxide dismutase) provided significant protection against palmitic acid toxicity.

Overexpression of catalase in insulin-producing cells reduced palmitic acid-induced ROS generation. ROS generation in RINm5F insulin-producing control cells as measured by the DCF fluorescence method was increased by about 40% in response to exposure to 100 μmol/l palmitic acid (Fig. 4). Overexpression of catalase in the peroxisomes and the cytosol, but not in the mitochondria, significantly reduced palmitic acid-induced (100 μmol/l) ROS generation.

Peroxisomes in rat islet cells, RINm5F insulin-producing cells, and HepG2 cells. Peroxisomes were clearly detectable by immunofluorescence as small green spots in primary rat β-cells, RINm5F insulin-producing cells, and HepG2 cells (supplementary Fig. S3). β-Cells isolated from rat pancreatic islets were identified by immunofluorescent staining of insulin; RINm5F cells were also positive for insulin. To quantify the density of peroxisomes in insulin-producing and hepatoma cells, the peroxisomes were counted in β-cells, RINm5F cells, and HepG2 cells after immunfluorescence staining of the peroxisomes by PMP-70 in 5–8 images (supplementary Fig. S4). The number of peroxisomes per cell was determined by the image analysis software Imaris (Bitplane, Zurich, Switzerland). The results clearly show that there were no significant differences in peroxisome density in hepatoma and in insulin-producing RINm5F cells as well as in primary rat β-cells.

Intracellular localization of the HyPer-Peroxi protein. To prove the intracellular localization of the HyPer protein targeted to the peroxisomes in RINm5F cells, fixed cells were stained for the peroxisomal membrane protein 70 (PMP-70). The fluorescence (504/520 nm) of the HyPer protein was clearly detectable as green spots after fixation with paraformaldehyde. Staining of the peroxisomes (PMP-70) showed a distinct colocalization with the HyPer-Peroxi protein (supplementary Fig. S5 *A–C*).

Subcellular site of H$_2$O$_2$ generation in insulin-producing cells following exposure to palmitic acid. In order to obtain more information about the nature of the reactive oxygen species and the intracellular site of ROS production after palmitic acid exposure, the HyPer protein, which is a specific sensor for H$_2$O$_2$, was expressed in either the peroxisomes (RINm5F-HyPer-Peroxi) or the mitochondria (RINm5F-HyPer-Mito) of RINm5F insulin-producing cells. The HyPer protein allows ratiometric measurement of H$_2$O$_2$ by fluorescence microscopy at two different wavelengths. In the false-colored overlay images, green staining corresponds to low, yellow to medium, and red to high H$_2$O$_2$ concentrations. After 24 h of exposure to palmitic acid, RINm5F-HyPer-Peroxi cells showed a strong
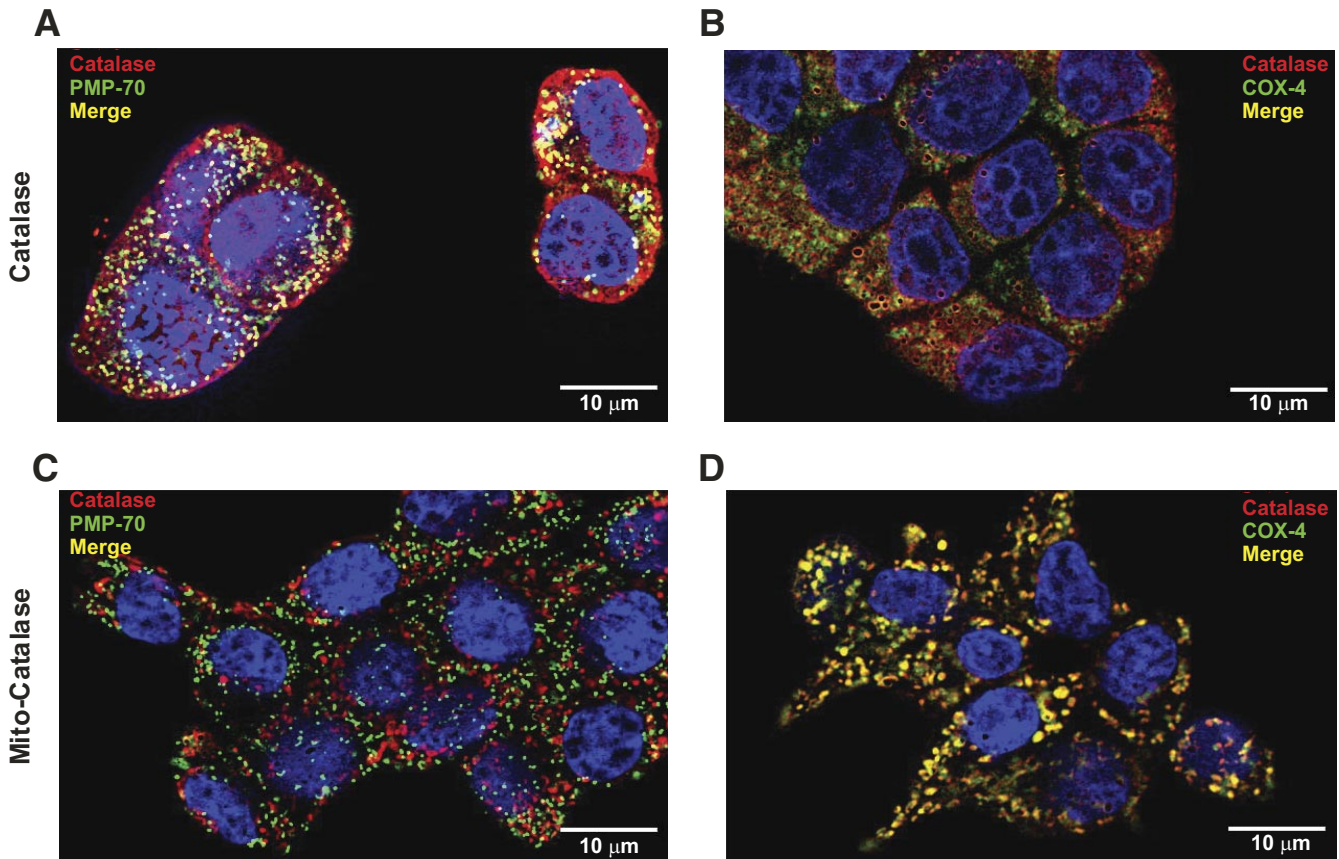
FIG. 2. Immunocytochemical staining for catalase, peroxisomes, and mitochondria in catalase or mitocatalase overexpressing RINm5F insulin-producing cells. RINm5F insulin-producing cells that overexpressed catalase in the cytosol (Catalase, A and B) or in the mitochondria (MitoCatalase, C and D) were seeded overnight on collagen-coated coverslips. After fixation with 4% paraformaldehyde, the cells were stained for catalase (red) and for the peroxisomal membrane protein 70 (PMP-70 green) or the mitochondrial respiratory chain enzyme cytochrome c-oxidase IV (COX-4 green) followed by nuclear counterstaining with DAPI (blue). To quantify the colocalization between catalase and the peroxisomes or mitochondria 20 images of two independent preparations were analyzed with the colocalization add-in of the CellR software (Olympus, Hamburg, Germany). The analyses showed that $56.2 \pm 3.3\%$ ($n = 58$) of catalase were localized in the peroxisomes (A) and $5 \pm 0.4\%$ ($n = 74$) in the mitochondria (B). For the MitoCatalase expressing cells, a proportion of $86.3 \pm 2.6\%$ ($n = 90$) of catalase was detected in the mitochondria (C) and $5.1 \pm 1.6\%$ ($n = 62$) in the peroxisomes (D). Data are means $\pm$ SEM of (n) individual cells. (A high-quality digital representation of this figure is available in the online issue.)
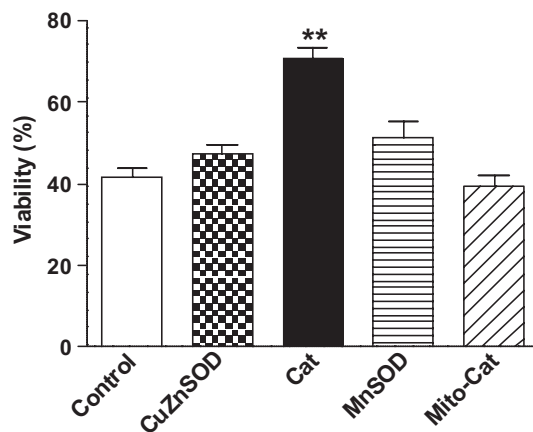

FIG. 3. Palmitic acid toxicity in RINm5F insulin-producing cells that overexpress different antioxidative enzymes. RINm5F cells that stably overexpressed the cytosolic antioxidative enzymes copper zinc superoxide dismutase (CuZnSOD) and catalase (Cat) or the mitochondrial antioxidative enzymes manganese superoxide dismutase (MnSOD) and catalase with a mitochondrial leader sequence (Mito-Cat) were incubated with palmitic acid (100 μmol/l) for 24 h; viability was determined by MTT assay. Mock-transfected RINm5F cells served as controls; untreated cells were set as 100% viability. Data are means ± SEM from five individual experiments. **$P < 0.01$ as compared with control cells (ANOVA/Dunnett test for multiple comparisons).
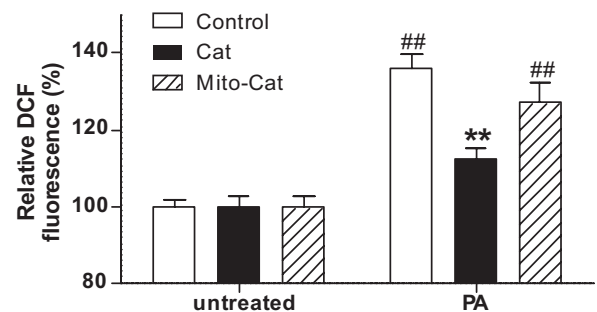

FIG. 4. Palmitic acid-induces production of reactive oxygen species in RINm5F insulin-producing cells that overexpress catalase in the cytosol (Cat) or in the mitochondria (Mito-Cat). To determine ROS generation, cells were loaded with 10 μmol/l of DCF-DA dye for 30 min and then cultured with 100 μmol/l palmitic acid for 24 h. DCF fluorescence was measured after 24 h and normalized to that of untreated cells. Data are means ± SEM from seven individual experiments. ##$P < 0.01$ as compared with untreated cells (t test, unpaired, two-tailed); **$P < 0.01$ as compared with control cells (ANOVA/Dunnett test for multiple comparisons).
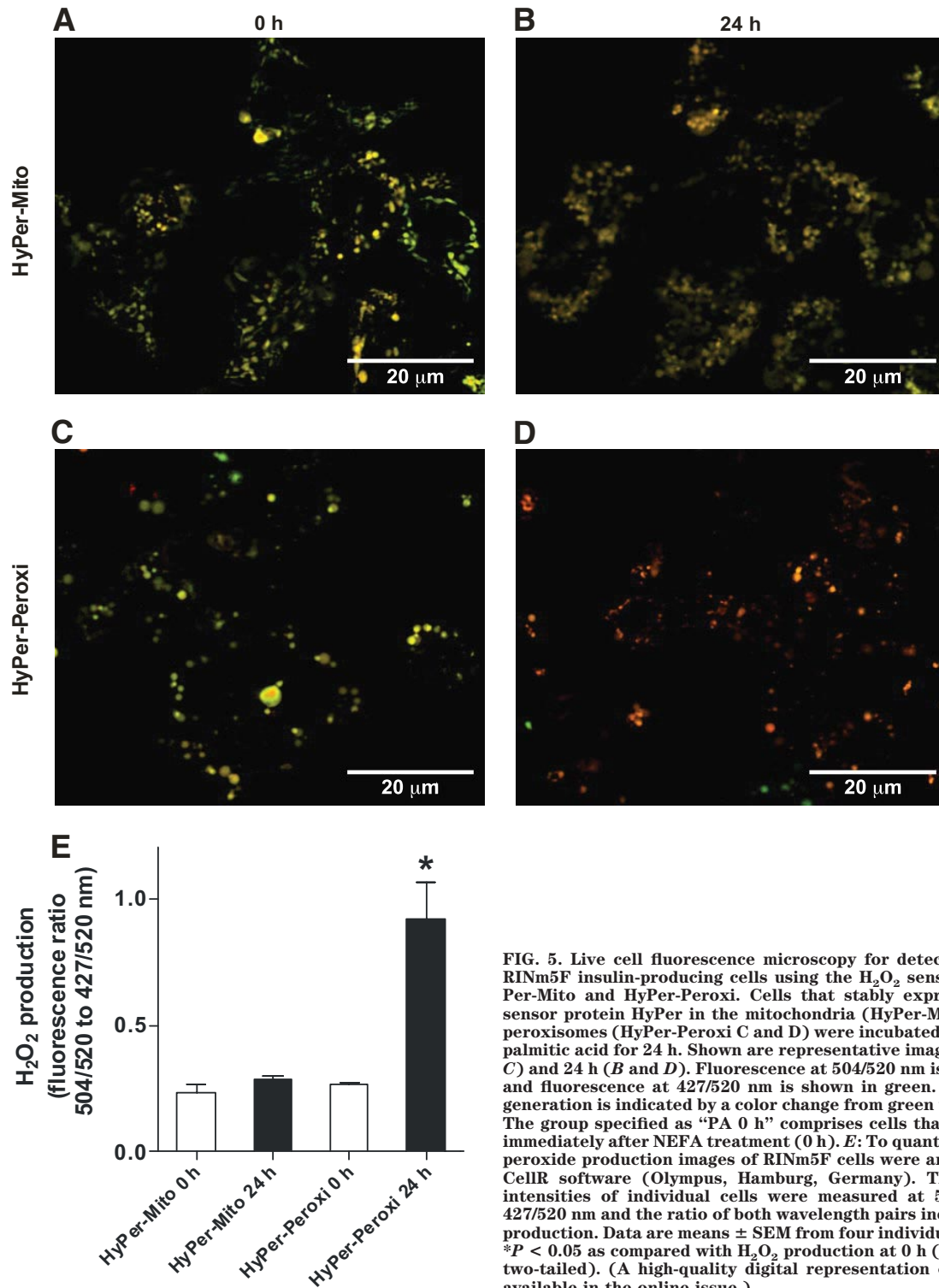
FIG. 5. Live cell fluorescence microscopy for detection of H_2O_2 in RINm5F insulin-producing cells using the H_2O_2 sensor proteins HyPer-Mito and HyPer-Peroxi. Cells that stably expressed the H_2O_2 sensor protein HyPer in the mitochondria (HyPer-Mito A and B) or peroxisomes (HyPer-Peroxi C and D) were incubated with 100 µmol/l palmitic acid for 24 h. Shown are representative images at 0 h (*A* and *C*) and 24 h (*B* and *D*). Fluorescence at 504/520 nm is depicted in red and fluorescence at 427/520 nm is shown in green. Increased H_2O_2 generation is indicated by a color change from green to yellow to red. The group specified as "PA 0 h" comprises cells that were analyzed immediately after NEFA treatment (0 h). *E*: To quantify the hydrogen peroxide production images of RINm5F cells were analyzed with the CellR software (Olympus, Hamburg, Germany). The fluorescence intensities of individual cells were measured at 504/520 nm and 427/520 nm and the ratio of both wavelength pairs indicates the H_2O_2 production. Data are means ± SEM from four individual experiments. *$P < 0.05$ as compared with H_2O_2 production at 0 h (*t* test, unpaired, two-tailed). (A high-quality digital representation of this figure is available in the online issue.)

shift toward red fluorescence (Fig. 5*C* and *D*). The quantification revealed a significant 240% increase of H_2O_2 production after a 24-h palmitic acid treatment (Fig. 5*E*). In contrast, the RINm5F-HyPer-Mito cells showed only a slight nonsignificant increase in red fluorescence, indicating a lower H_2O_2 concentration in the mitochondria relative to the peroxisomes (Fig. 5*A*, *B*, and *E*). RINm5F-HyPer-Peroxi and RINm5F-HyPer-Mito cells incubated without palmitic acid under control conditions for 24 h showed no changes in fluorescence signals (data not shown).

The key finding of H_2O_2 generation in the peroxisomes of RINm5F cells after exposure to palmitic acid was confirmed in primary rat islet cells. Single rat islet cells were lentivirally transduced with Hyper-Peroxi cDNA and incubated with palmitic acid for 24 h. In the palmitic acid treated islet cells a clear shift toward red fluorescence was detectable, which corresponds to a higher H_2O_2 concentration in comparison with untreated cells (Fig. 6). The fluorescence shift of single cells was quantified with the CellR software (Olympus, Hamburg, Germany). Palmitic acid treatment induced a significant 125% increase of H_2O_2
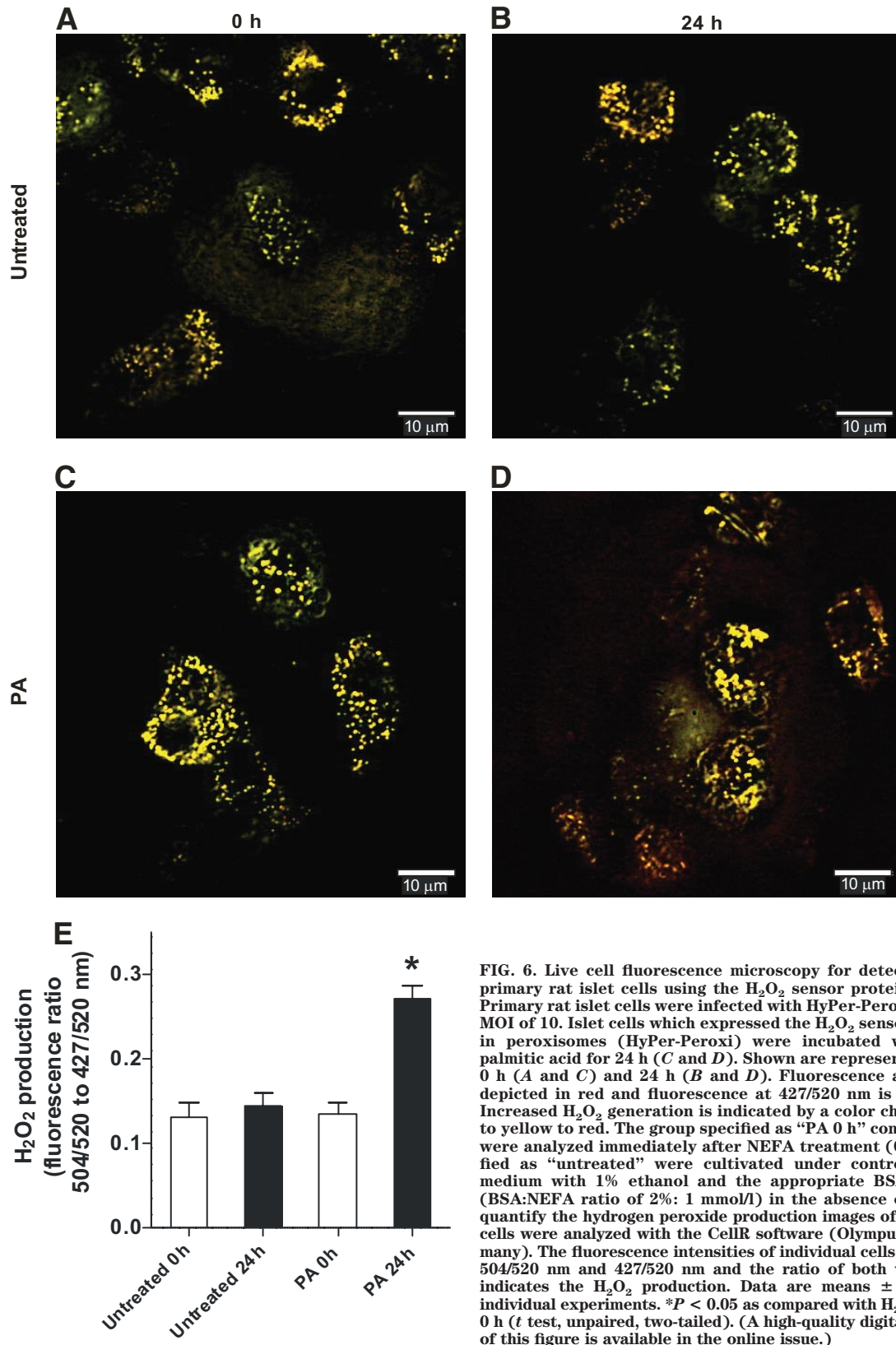
FIG. 6. Live cell fluorescence microscopy for detection of H_2O_2 in primary rat islet cells using the H_2O_2 sensor protein HyPer-Peroxi. Primary rat islet cells were infected with HyPer-Peroxi lentivirus at a MOI of 10. Islet cells which expressed the H_2O_2 sensor protein HyPer in peroxisomes (HyPer-Peroxi) were incubated with 500 μmol/l palmitic acid for 24 h (C and D). Shown are representative images at 0 h (A and C) and 24 h (B and D). Fluorescence at 504/520 nm is depicted in red and fluorescence at 427/520 nm is shown in green. Increased H_2O_2 generation is indicated by a color change from green to yellow to red. The group specified as "PA 0 h" comprises cells that were analyzed immediately after NEFA treatment (0 h). Cells specified as "untreated" were cultivated under control conditions in medium with 1% ethanol and the appropriate BSA concentration (BSA:NEFA ratio of 2%: 1 mmol/l) in the absence of NEFAs. E: To quantify the hydrogen peroxide production images of primary rat islet cells were analyzed with the CellR software (Olympus, Hamburg, Germany). The fluorescence intensities of individual cells was measured at 504/520 nm and 427/520 nm and the ratio of both wavelength pairs indicates the H_2O_2 production. Data are means ± SEM from four individual experiments. *$P < 0.05$ as compared with H_2O_2 production at 0 h (t test, unpaired, two-tailed). (A high-quality digital representation of this figure is available in the online issue.)

production in comparison with the control condition (Fig. 6E).

Quantification of H_2O_2 generation in insulin-producing cells following exposure to palmitic acid. Differences in peroxisomal and mitochondrial H_2O_2 concentration after 24-h exposure to palmitic acid were quantified spectrofluorometrically. Treatment with 100 μmol/l palmitic acid induced a significantly higher rate of H_2O_2 production in both the peroxisomes and the mitochondria of control RINm5F cells than did treatment with 50 μmol/l palmitic acid (Fig. 7A and B). At 100 μmol/l palmitic acid, there was a tendency for a greater increase
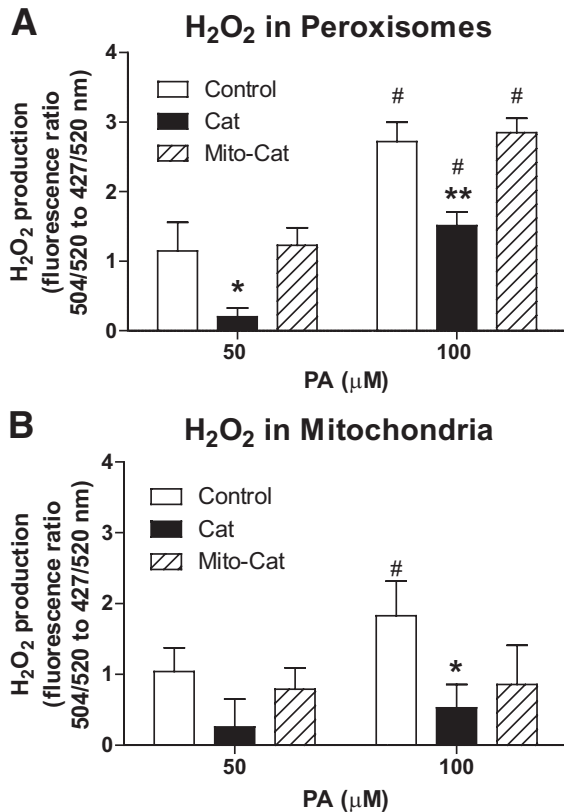
A

H₂O₂ in Peroxisomes

B

H₂O₂ in Mitochondria

FIG. 7. Localization of H$_2$O$_2$ production in RINm5F insulin-producing cells after palmitic acid treatment. Cells that stably expressed the H$_2$O$_2$ sensor protein HyPer in peroxisomes (*A*) or mitochondria (*B*) and catalase in the cytosol (Cat) or mitochondria (Mito-Cat) were treated with 50 or 100 μmol/l palmitic acid for 24 h. The fluorescence ratio (504/520 nm to 427/520 nm), which is an indicator of H$_2$O$_2$ production, was measured spectrofluorometrically. Shown are the changes in the fluorescence ratios after 24 h normalized to the fluorescence ratios of untreated cells. Data are means ± SEM from 10 individual experiments. #$P < 0.05$ vs. untreated cells (0 μmol/l PA), *$P < 0.05$, **$P < 0.01$ vs. control cells (ANOVA/Dunnett test for multiple comparisons).

FIG. 8. Localization of H$_2$O$_2$ production in INS-1E insulin-producing cells after palmitic acid treatment. Cells that stably expressed the H$_2$O$_2$ sensor protein HyPer in the peroxisomes or the mitochondria were treated with 500 μmol/l palmitic acid for 24 h. The fluorescence ratio (504/520 nm to 427/520 nm), which is an indicator of H$_2$O$_2$ production, was measured spectrofluorometrically. Shown are the changes in the fluorescence ratios after 24 h normalized to the fluorescence ratios of untreated cells. Data are means ± SEM from 14 individual experiments. *$P < 0.05$ vs. HyPer-Peroxi; ##< 0.01 vs. untreated cells (*t* test, unpaired, two-tailed).

Overall, the data showed that overexpression of catalase in peroxisomes and cytosol reduced H$_2$O$_2$ generation in the peroxisomes and, to a lesser extent, in the mitochondria. In contrast, overexpression of catalase in the mitochondria had no significant effect on H$_2$O$_2$ production in either organelle (compare Fig. 7*A* and *B*).

DISCUSSION

The present data clearly show that NEFA toxicity increases with increasing chain length. NEFAs are oxidized not only in the mitochondria, but also in the peroxisomes. Fatty acid β-oxidation is a property of peroxisomes in most, if not all, organisms (27). Moreover, in yeast and plants, peroxisomes are the sole sites of fatty acid β-oxidation (44). One product of peroxisomal β-oxidation is H$_2$O$_2$, whereas mitochondrial β-oxidation generates reducing equivalents (27,28). Mitochondrial β-oxidation is tightly coupled to the respiratory chain and oxidative phosphorylation. It provides acetyl-CoA for further oxidation in the TCA cycle and ensures the production of ATP, which is not an apparent function of peroxisomal β-oxidation. In peroxisomal β-oxidation, the initial step generates H$_2$O$_2$ and energy is lost as heat. Peroxisomal β-oxidation results in chain shortening of long- and very long-chain fatty acids, which are poor substrates for mitochondrial β-oxidation. The shortened fatty acids are subsequently transported to the mitochondria in a carnitine-dependent manner for further degradation (27,28).

The observation of the chain length-dependent increase in the toxicity of saturated fatty acids to insulin-producing cells prompted us to study the role of oxygen free radicals generated by peroxisomal β-oxidation as mediators of lipotoxicity. In the first step of peroxisomal β-oxidation, FAD-containing acyl-CoA oxidase introduces a double bond at the β-position of the fatty-acyl-CoA ester and the hydrogen atoms are transferred to molecular oxygen to yield H$_2$O$_2$ (28). Remarkably, in rat liver, for example, about 20% of total oxygen consumption is accounted for peroxisomal oxidase activity (45). For the detoxification of H$_2$O$_2$, the oxidoreductase catalase, which has a high turnover rate, is expressed in the peroxisomes of most tissues (28), but not in those of pancreatic β-cells (29,30). This low catalase enzyme activity could also be found in RINm5F cells, which makes these cells well suited as model cells for H$_2$O$_2$-mediated lipotoxicity.

of the peroxisomal as compared with the mitochondrial H$_2$O$_2$ production in RINm5F cells (Fig. 7*A* and *B*). In INS-1E cells, the H$_2$O$_2$ production was even significantly higher in the peroxisomes than in the mitochondria after palmitic acid treatment (Fig. 8).

Additional information about the intracellular site of H$_2$O$_2$ production after palmitic acid exposure was obtained by overexpressing the H$_2$O$_2$ detoxifying enzyme catalase either in the peroxisomes and the cytosol or in the mitochondria of RINm5F-HyPer-Peroxi and RINm5F-HyPer-Mito cells, respectively. Catalase expression in the peroxisomes and cytosol of RINm5F-HyPer-Peroxi cells reduced H$_2$O$_2$ production significantly in the presence of 50 and 100 μmol/l palmitic acid as compared with control cells, whereas overexpression of catalase in the mitochondria did not significantly reduce H$_2$O$_2$ production in the peroxisomes (Fig. 7*A*).

Overexpression of catalase in the peroxisomes and the cytosol significantly reduced the mitochondrial H$_2$O$_2$ concentration in response to incubation with 100 μmol/l (and to a lesser extent with 50 μmol/l) palmitic acid as compared with control cells. Overexpression of catalase in the mitochondria did not significantly affect mitochondrial production of H$_2$O$_2$ even though there was a tendency toward a reduction at 100 μmol/l palmitic acid (Fig. 7*B*).
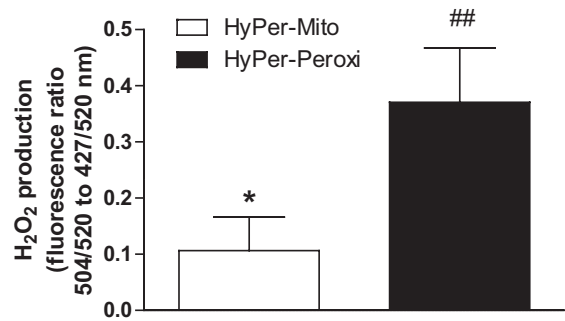
Experiments with insulin-producing cells overexpressing antioxidative enzymes showed that only cytosolic catalase provided protection against palmitic acid-induced toxicity; mitochondrial catalase was not protective. The superoxide radical detoxifying isoenzymes MnSOD and CuZnSOD were also not protective, indicating that the formation of superoxide radicals does not play as crucial a role in lipotoxicity as does the formation of H_2O_2. Indeed, determination of ROS production by DCF fluorescence measurements provided support for this hypothesis by showing a reduction in ROS generation in insulin-producing cells that overexpressed catalase in the peroxisomes and the cytosol, but not in the mitochondria. Using the H_2O_2-sensitive HyPer protein as a novel, specific method for detecting H_2O_2, we clearly identified H_2O_2 as the main reactive oxygen species formed during palmitic acid treatment. To determine the subcellular site of H_2O_2 formation, the HyPer protein was fused to a peroxisome- or a mitochondrion-targeting sequence to allow organelle-specific expression.

These experiments show that peroxisomes were a major site of H_2O_2 formation in insulin-producing cells, whereas the mitochondria were a minor site. Primary rat islet cells are well equipped with peroxisomes, and also showed an increased peroxisomal H_2O_2 formation in response to palmitic acid, as demonstrated in this study.

An additional argument for this hypothesis is the fact that overexpression of catalase in the peroxisomes and the cytosol (RINm5F-Cat) significantly reduced H_2O_2 production not only in the peroxisomes, but also in the mitochondria, though catalase was not overexpressed in the latter organelle. H_2O_2 as a membrane-permeable ROS (23,24) can diffuse from its site of generation in the peroxisome into the mitochondria where it is detected through the HyPer-Mito protein. Thus, the source of the elevated H_2O_2 concentration detected in the mitochondria is at least in part H_2O_2-generated in the peroxisomes.

However, in contrast to the peroxisomes in other cell types, insulin-producing cells do not appear to express catalase mRNA or protein (29,30). This lack of catalase expression leaves insulin-producing cells badly protected against potentially hazardous effects of H_2O_2 generated through peroxisomal β-oxidation. Mitochondrial β-oxidation may not be able to cope with the elevated levels of NEFAs that are associated with obesity and type 2 diabetes, resulting in a higher proportion of fatty acids being metabolized through peroxisomal β-oxidation, leading to increased H_2O_2 formation. The membrane-permeable H_2O_2 could leave the peroxisomes and harm insulin biosynthesis and secretion (11,46,47), as has been shown for insulin-secreting cells after exposure to high NEFA concentrations for extended periods (15). The results of the present study indicate that ROS generated in the peroxisomes are the major cause of lipotoxicity-mediated β-cell dysfunction. This does not detract from the fact that mitochondrial ROS formation may contribute to this phenomenon, in particular with respect to direct negative effects on mitochondrial function.

NADPH oxidase activation could also be a source of long-chain fatty acid-mediated superoxide radical generation (22) that has been postulated to cause lipotoxicity in insulin-producing cells (15,48). Palmitic acid has been shown to activate this plasma membrane enzyme in aortic smooth muscle and endothelial cells in a protein kinase C-dependent manner, leading to superoxide radical formation (49). In insulin-producing cells, palmitic acid can induce superoxide radical formation along with increased expression of the NADPH oxidase p47^{phox} subunit (15,48,50). However, data from the present study indicated that cytosolic CuZnSOD did not protect insulin-producing cells against palmitic acid-induced toxicity, suggesting that an increased rate of superoxide radical formation per se is insufficient to explain NEFA-induced lipotoxicity.

Thus, we hypothesize that NEFA-induced lipotoxicity is mediated by H_2O_2 generated during peroxisomal β-oxidation of palmitic acid as the physiologically most abundant long-chain saturated fatty acid. This provides an interesting new concept for lipid-induced glucose intolerance in obesity and diabetic hyperglycemia as a result of β-cell dysfunction in patients with type 2 diabetes. The lack of catalase expression in pancreatic β-cell peroxisomes (29,30) explains the exceptional susceptibility of pancreatic β-cells to lipotoxicity (14,15,23).

REFERENCES

1. Boden G: Role of fatty acids in the pathogenesis of insulin resistance and NIDDM. Diabetes 1997;46:3–10
2. DeFronzo RA: Lilly lecture 1987. The triumvirate: β-cell, muscle, liver. A collusion responsible for NIDDM. Diabetes 1988;37:667–687
3. Carpentier A, Mittelman SD, Lamarche B, Bergman RN, Giacca A, Lewis GF. Acute enhancement of insulin secretion by FFA in humans is lost with prolonged FFA elevation. Am J Physiol 1999;276:E1055–E1066
4. Kashyap S, Belfort R, Gastaldelli A, Pratipanawatr T, Berria R, Pratipanawatr W, Bajaj M, Mandarino L, DeFronzo R, Cusi K. A sustained increase in plasma free fatty acids impairs insulin secretion in nondiabetic subjects genetically predisposed to develop type 2 diabetes. Diabetes 2003;52:2461–2474
5. Paolisso G, Gambardella A, Amato L, Tortoriello R, D'Amore A, Varricchio M, D'Onofrio F. Opposite effects of short- and long-term fatty acid infusion on insulin secretion in healthy subjects. Diabetologia 1995;38:1295–1299
6. Butler AE, Janson J, Bonner-Weir S, Ritzel R, Rizza RA, Butler PC. β-cell deficit and increased β-cell apoptosis in humans with type 2 diabetes. Diabetes 2003;52:102–110
7. Clark A, Wells CA, Buley ID, Cruickshank JK, Vanhegan RI, Matthews DR, Cooper GJ, Holman RR, Turner RC. Islet amyloid, increased A-cells, reduced B-cells and exocrine fibrosis: quantitative changes in the pancreas in type 2 diabetes. Diabetes Res 1988;9:151–159
8. Rahier J, Guiot Y, Goebbels RM, Sempoux C, Henquin JC. Pancreatic β-cell mass in European subjects with type 2 diabetes. Diabetes Obes Metab 2008;10(Suppl 4):32–42
9. Gordon ES. Non-esterified fatty acids in the blood of obese and lean subjects. Am J Clin Nutrition 1960;8:740–747
10. Poitout V, Robertson RP. Minireview: Secondary β-cell failure in type 2 diabetes–a convergence of glucotoxicity and lipotoxicity. Endocrinology 2002;143:339–342
11. Zhou YP, Grill VE. Long-term exposure of rat pancreatic islets to fatty acids inhibits glucose-induced insulin secretion and biosynthesis through a glucose fatty acid cycle. J Clin Invest 1994;93:870–876
12. Azevedo-Martins AK, Monteiro AP, Lima CL, Lenzen S, Curi R. Fatty acid-induced toxicity and neutral lipid accumulation in insulin-producing RINm5F cells. Toxicol In Vitro 2006;20:1106–1113
13. Cnop M, Hannaert JC, Hoorens A, Eizirik DL, Pipeleers DG. Inverse relationship between cytotoxicity of free fatty acids in pancreatic islet cells and cellular triglyceride accumulation. Diabetes 2001;50:1771–1777
14. Cnop M. Fatty acids and glucolipotoxicity in the pathogenesis of type 2 diabetes. Biochem Soc Trans 2008;36:348–352

15. Newsholme P, Keane D, Welters HJ, Morgan NG. Life and death decisions of the pancreatic β-cell: the role of fatty acids. Clin Sci (Lond) 2007;112:27–42
16. Cnop M, Igoillo-Esteve M, Cunha DA, Ladriere L, Eizirik DL. An update on lipotoxic endoplasmic reticulum stress in pancreatic β-cells. Biochem Soc Trans 2008;36:909–915
17. Cunha DA, Hekerman P, Ladriere L, Bazarra-Castro A, Ortis F, Wakeham MC, Moore F, Rasschaert J, Cardozo AK, Bellomo E, Overbergh L, Mathieu C, Lupi R, Hai T, Herchuelz A, Marchetti P, Rutter GA, Eizirik DL, Cnop M. Initiation and execution of lipotoxic ER stress in pancreatic β-cells. J Cell Sci 2008;121:2308–2318
18. Lai E, Bikopoulos G, Wheeler MB, Rozakis-Adcock M, Volchuk A. Differential activation of ER stress and apoptosis in response to chronically elevated free fatty acids in pancreatic β-cells. Am J Physiol Endocrinol Metab 2008;294:E540–E550
19. Berne C. The metabolism of lipids in mouse pancreatic islets. The oxidation of fatty acids and ketone bodies. Biochem J 1975;152:661–666
20. Lenzen S, Panten U. 2-oxocarboxylic acids and function of pancreatic islets in obese-hyperglycaemic mice. Insulin secretion in relation to 45Ca uptake and metabolism. Biochem J 1980;186:135–144
21. Panten U, Lenzen S. Alterations in energy metabolism of secretory cells. In The Energetics of Secretion Responses. Boca Raton, FL, CRC Press, 1988
22. Schonfeld P, Wojtczak L. Fatty acids as modulators of the cellular production of reactive oxygen species. Free Radic Biol Med 2008;45:231–241
23. Lenzen S. Oxidative stress: the vulnerable β-cell. Biochem Soc Trans 2008;36:343–347
24. Halliwell B, Gutteridge JMC. Free Radicals in Biology and Medicine. New York, Oxford University Press, 2007
25. El-Assaad W, Buteau J, Peyot ML, Nolan C, Roduit R, Hardy S, Joly E, Dbaibo G, Rosenberg L, Prentki M. Saturated fatty acids synergize with elevated glucose to cause pancreatic β-cell death. Endocrinology 2003;144:4154–4163
26. Hellemans K, Kerckhofs K, Hannaert JC, Martens G, Van Veldhoven P, Pipeleers D. Peroxisome proliferator-activated receptor alpha-retinoid X receptor agonists induce β-cell protection against palmitate toxicity. FEBS J 2007;274:6094–6105
27. Kunau WH, Dommes V, Schulz H. β-oxidation of fatty acids in mitochondria, peroxisomes, and bacteria: a century of continued progress. Prog Lipid Res 1995;34:267–342
28. Dansen TB, Wirtz KW. The peroxisome in oxidative stress. IUBMB Life 2001;51:223–230
29. Lenzen S, Drinkgern J, Tiedge M. Low antioxidant enzyme gene expression in pancreatic islets compared with various other mouse tissues. Free Radic Biol Med 1996;20:463–466
30. Tiedge M, Lortz S, Drinkgern J, Lenzen S. Relation between antioxidant enzyme gene expression and antioxidative defense status of insulin-producing cells. Diabetes 1997;46:1733–1742
31. Asfari M, Janjic D, Meda P, Li G, Halban PA, Wollheim CB. Establishment of 2-mercaptoethanol-dependent differentiated insulin-secreting cell lines. Endocrinology 1992;130:167–178
32. Lortz S, Gurgul-Convey E, Lenzen S, Tiedge M. Importance of mitochondrial superoxide dismutase expression in insulin-producing cells for the toxicity of reactive oxygen species and proinflammatory cytokines. Diabetologia 2005;48:1541–1548
33. Gurgul E, Lortz S, Tiedge M, Jorns A, Lenzen S. Mitochondrial catalase overexpression protects insulin-producing cells against toxicity of reactive oxygen species and proinflammatory cytokines. Diabetes 2004;53:2271–2280
34. Claiborne A. Catalase activity. In CRC Handbook of Methods for Oxygen Radical Research. Greenwald RA, Ed. Boca Raton, FL, CRC Press, 1985, p. 283–284
35. Cornu M, Modi H, Kawamori D, Kulkarni RN, Joffraud M, Thorens B. Glucagon-like peptide-1 (GLP-1) increases β-cell glucose competence and proliferation by translational induction of insulin-like growth factor-1 receptor (IGF-1R) expression. J Biol Chem 2010;285:10538–10545
36. Mosmann T. Rapid colorimetric assay for cellular growth and survival: application to proliferation and cytotoxicity assays. J Immunol Methods 1983;65:55–63
37. Darzynkiewicz Z, Bruno S, Del Bino G, Gorczyca W, Hotz MA, Lassota P, Traganos F. Features of apoptotic cells measured by flow cytometry. Cytometry 1992;13:795–808
38. Rosenkranz AR, Schmaldienst S, Stuhlmeier KM, Chen W, Knapp W, Zlabinger GJ. A microplate assay for the detection of oxidative products using 2′,7′-dichlorofluorescin-diacetate. J Immunol Methods 1992;156:39–45
39. Belousov VV, Fradkov AF, Lukyanov KA, Staroverov DB, Shakhbazov KS, Terskikh AV, Lukyanov S. Genetically encoded fluorescent indicator for intracellular hydrogen peroxide. Nat Methods 2006;3:281–286
40. de Hoop MJ, Ab G. Import of proteins into peroxisomes and other microbodies. Biochem J 1992;286(Pt 3):657–669
41. Subramani S. Protein import into peroxisomes and biogenesis of the organelle. Annu Rev Cell Biol 1993;9:445–478
42. Zufferey R, Dull T, Mandel RJ, Bukovsky A, Quiroz D, Naldini L, Trono D. Self-inactivating lentivirus vector for safe and efficient in vivo gene delivery. J Virol 1998;72:9873–9880
43. Sastry L, Johnson T, Hobson MJ, Smucker B, Cornetta K. Titering lentiviral vectors: comparison of DNA, RNA and marker expression methods. Gene Ther 2002;9:1155–1162
44. Wanders RJ, Waterham HR. Biochemistry of mammalian peroxisomes revisited. Annu Rev Biochem 2006;75:295–332
45. Reddy JK, Mannaerts GP. Peroxisomal lipid metabolism. Annu Rev Nutr 1994;14:343–370
46. Akesson B, Lundquist I. Nitric oxide and hydroperoxide affect islet hormone release and Ca(2+) efflux. Endocrine 1999;11:99–107
47. Maechler P, Jornot L, Wollheim CB. Hydrogen peroxide alters mitochondrial activation and insulin secretion in pancreatic β cells. J Biol Chem 1999;274:27905–27913
48. Morgan D, Oliveira-Emilio HR, Keane D, Hirata AE, Santos da Rocha M, Bordin S, Curi R, Newsholme P, Carpinelli AR. Glucose, palmitate and pro-inflammatory cytokines modulate production and activity of a phagocyte-like NADPH oxidase in rat pancreatic islets and a clonal β cell line. Diabetologia 2007;50:359–369
49. Inoguchi T, Li P, Umeda F, Yu HY, Kakimoto M, Imamura M, Aoki T, Etoh T, Hashimoto T, Naruse M, Sano H, Utsumi H, Nawata H. High glucose level and free fatty acid stimulate reactive oxygen species production through protein kinase C–dependent activation of NAD(P)H oxidase in cultured vascular cells. Diabetes 2000;49:1939–1945
50. Lambertucci RH, Hirabara SM, Silveira Ldos R, Levada-Pires AC, Curi R, Pithon-Curi TC. Palmitate increases superoxide production through mitochondrial electron transport chain and NADPH oxidase activity in skeletal muscle cells. J Cell Physiol 2008;216:796–804